http://onlinelibrary.wiley.com/enhanced/doi/10.1002/bem.20608/

DOI: 10.1002/bem.20608

In vitro study of the effects of ELF electric fields on gene expression in human epidermal cells

Jean-Francois Collard, Benjamin Mertens, Maurice Hinsenkamp

Abstract

An acceleration of differentiation, at the expense of proliferation, is observed after exposure of various biological models to low frequency and low amplitude electric and electromagnetic fields. Following these results showing significant modifications, we try to identify the biological mechanism involved at the cell level through microarray screening. For this study, we use epidermis cultures harvested from human abdominoplasty. Two platinum electrodes are used to apply the electric signal. The gene expressions of 38,500 well-characterized human genes are analyzed using Affymetrix® microarray U133 Plus 2.0 chips. The protocol is repeated on three different patients. After three periods of exposure, a total of 24 chips have been processed. After the application of ELF electric fields, the microarray analysis confirms a modification of the gene expression of epidermis cells. Particularly, four up-regulated genes (DKK1, TXNRD1, ATF3, and MME) and one down-regulated gene (MACF1) are involved in the regulation of proliferation and differentiation. Expression of these five genes was also confirmed by real-time rtPCR in all samples used for microarray analysis. These results corroborate an acceleration of cell differentiation at the expense of cell proliferation. Bioelectromagnetics 32:28–36, 2011. © 2010 Wiley-Liss, Inc.

INTRODUCTION

Our laboratory observed the following biological responses on various models of growing or healing bone tissues after exposure to low frequency and low amplitude electromagnetic fields performed with Helmholtz coils, and an induced current characterized by a carrier frequency of 4 KHz (pulse train) modulated by a fundamental wave of 15 Hz.

For mice embryos in vitro: A series of right and left limb buds (control and stimulated) from the same embryos were cultivated in a semi-synthetic culture medium for 6 days. Comparison of histological techniques (Toluidine blue, Hale's colloidal iron method) shows for each staining, a statistical increase in the concentration of acid glycosaminoglycans [Hinsenkamp and Rooze, 1982; Rooze and Hinsenkamp, 1982; Hinsenkamp, 1994].

For tibia and metatarsal bones of chicken embryos in vivo: White leghorn eggs incubated for 4 days were divided into two groups, control and stimulated, and placed in the same incubator. After sampling, bulk skeletal double staining following Watson's method was used to measure the total length of bone rudiment and the length of the primary ossification point. The statistical analysis

shows a significant increase in the total length and also a relative acceleration in the ossification process of the primary ossification point [Rooze and Hinsenkamp, 1985; Hinsenkamp, 1994].

For quail embryos: 178 quail embryos were placed in a specific area between Helmholtz coils and a relation was observed between the different amplitudes of the local electric field and the ossification ratio. For this protocol, we used the same staining and methods as for the chicken embryos [Hinsenkamp et al., 1985a; Hinsenkamp, 1994].

These results and clinical studies [Hinsenkamp et al., 1984, 1985b, 1993a,b; Hinsenkamp, 1994] are all in agreement with an accelerated differentiation of the cartilaginous matrix preceding the ossification.

In the present protocol, we use cultures of epidermis on deepidermized human skin. This model of epidermal growth provides a simplified and well-characterized model to study the biological effects of low-frequency electric fields. This model uses a 40 Hz pulsed asymmetric charge-balanced carrier signal modulated by a fundamental frequency of 0.125 Hz and transmitted by two platinum electrodes [Jercinovic et al., 1996; Hinsenkamp et al., 1997]. On the stimulated cultures, the results showed:

- a decrease in growth area surrounding the explants;
- better stratification with an increased number of cell layers;
- a decreased percentage of cells marked with [H3]-thymidine.

Planimetry, histologic examination, and [H3]-thymidine labeling results published by Hinsenkamp et al. 1997 suggested that low-frequency pulsed electrical stimulation had influenced differentiation of the epidermal culture because better structured and mature epidermal layers were formed in areas around stimulated explants. This was achieved at the expense of the proliferation of the keratinocytes culture as the number of mitoses decreased in parallel with the growth area.

It is interesting to note that results obtained in the study using low-frequency pulsed electric current reproduced the same conclusion we obtained in studies on the effects of electromagnetic fields on bone tissue. Bone studies showed faster maturation of the cartilaginous matrix associated with an acceleration of the ossification in embryonic tissue models and on fracture callus when exposed to an electromagnetic field [Hinsenkamp, 1994]. These results confirm the acceleration of differentiation at the expense of proliferation observed in vivo on different organisms (human and animal) and in vitro on tissue and cell cultures with the same kind of electric signal.

Considering the very coherent response of our biological models to specific low frequencies and low-amplitude, asymmetric, charge-balanced, pulse-train modulated electric or electromagnetic fields, we try to identify the mechanism involved at the cell level through microarray screening.

MATERIALS AND METHODS

Biological Model

Human epidermal explants were cultured at an air–liquid interface on decellularized human dermal supports (resulting in cell stratification similar to the in vivo physiological epidermal development). Two platinum electrodes are used to apply the electric signal. Pairs of samples from the same skin

donors were prepared for the study. In each pair, one sample is exposed to electrical stimulation for 40 min per day for 11 days and the other is used as control.

The in vitro model is prepared with skin harvested from human abdominoplasty after plastic surgery. The dermal support preparation includes: removal of epidermis, 20 successive freeze-thaw cycles of the remaining dermis, gamma radiation (7 KGy), and cutting of the dermis in a 60 mm × 30 mm rectangle. For epidermis explants, a thin layer of epidermis is removed from the skin with a Wagner's dermatome. Punch biopsy is used to remove a 3 mm circle of the epidermis layer.

The model is completed by the culture medium and foam on which the dermal support lies. Six epidermal explants, 3 mm in diameter, are placed on the dermal support. After 3 days, when the explants are attached to the dermal support, two platinum electrodes are placed on each side and are used to apply the electric signal (Fig. 1).

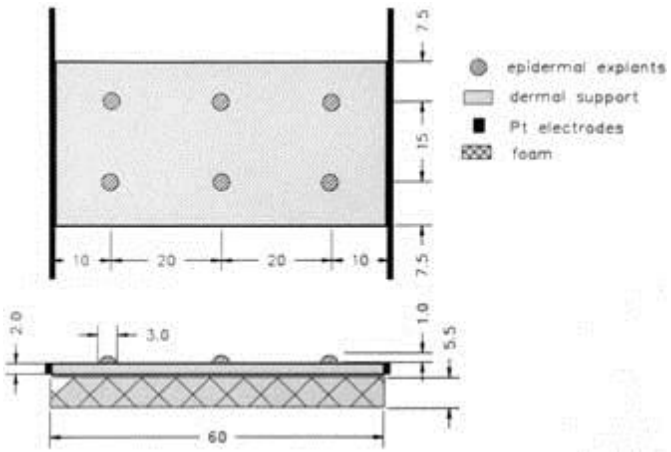

Figure 1. In vitro model. Six epidermal explants placed on the dermal support. The culture medium and two platinum electrodes complete the model.

Culture medium is composed of Dulbecco's modified Eagle medium and Ham's F12 nutrient mixture (3:1 v/v), 10% fetal calf serum, 6 µg/ml gentamicin, 50 U/50 µg penicillin/streptomycin, 0.25 µg/ml fungizon, and 0.45 µg/ml hydrocortisone. The culture medium is changed in each dish every 48 h. Eighty-four explants of the same patient are distributed on 14 dermal supports.

The control and stimulated groups are placed inside the incubator without stimulation for 3 days to allow rest and explant attachment to dermal support. We realized a control sample before this 3-day period at J−3, and after at J1. We collected three other control samples at J4, J7, and J12 and three stimulated samples at J4, J7, and J12, at days 4, 7, and 12, respectively (Fig. 2). To obtain enough total RNA for microarray and real-time reverse transcriptase polymerase chain reaction (real-time rtPCR) experimentation, 12 explants are sampled and pooled for RNA extraction under each sample condition. To make a link with the previous results [Jercinovic et al., 1996; Hinsenkamp et al., 1997] and validate the success of the biological and electrical stimulation protocols, the same procedure was followed including the culture duration of 15 days.

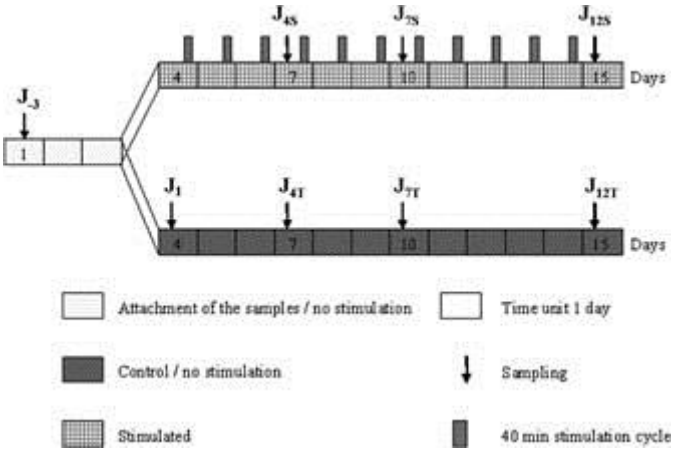

Figure 2. Study design. First control sample (J−3) and second control sample (J1) are made before and after the 3-day attachment period. We analyzed three other control samples at J4, J7, and J12 and three stimulated samples at J4, J7, and J12, at days 4, 7, and 12, respectively.

All Petri dishes (control and stimulated) are placed in the same incubator (37 ± 0.3 °C, 5% CO2). Temperature of culture medium was checked before and after stimulation with a digital thermocouple thermometer, Fluke 52 dual input (Fluke, Everett, WA). Two T-type hypodermic probes were used, one for the control Petri dish culture medium and the other for stimulated box culture medium. The incubator had not been opened between the pre- and post-stimulation measurements. No modification of the culture medium temperature (36.0 ± 0.32 °C) had been observed in the control and stimulated Petri dishes before and after stimulation.

Electrical Stimulation Pattern

The output of the generator consists of a biphasic, asymmetric, charge-balanced current stimuli, with a repetition frequency of 40 Hz modulated by a fundamental frequency of 0.125 Hz. The stimulus is repeated during 4 s followed by a 4 s break, for 40 min/day for 11 days. Electrical stimulation is applied through two platinum (Pt) electrodes (50 mm × 2 mm × 0.5 mm) in contact with the dermal support.

The generator output current amplitude is 20 mA peak and consists of a current generator and a 2.1 µF capacitor connected in series. By measuring the time constant of the potential (V) at the output of the generator, we may assimilate the dermal support to a pure resistance. The time constant measured is 430 µs, and Tau = RC gives us directly the resistor value (200 Ohms), which is the same result obtained with an electronic multimeter. Also, by adding a 200 Ohms electronic resistor in series, the time constant has been doubled.

Figure 3 shows the value of the electric field at the peak current amplitude of 20 mA (including the culture medium, foam, and dermis). The electric field at any point is measured using needles. These measurements are analyzed using COMSOL simulation software (Stockholm, Sweden), which provides maps of an electric field, the current distribution, and the voltage at any point. The COMSOL simulation validation is made by comparing electrical potential measurements at any point. The maximum electric field value around the electrode is 400 V/m. From the position of the six explants of epidermis (Fig. 1), the explants receive an electric field close to 275 V/m. The simulation also

shows the current distribution between the dermis and the environment. Variation of electric current is uniform and 20% of current density goes through the dermis, and 80% through the culture medium.

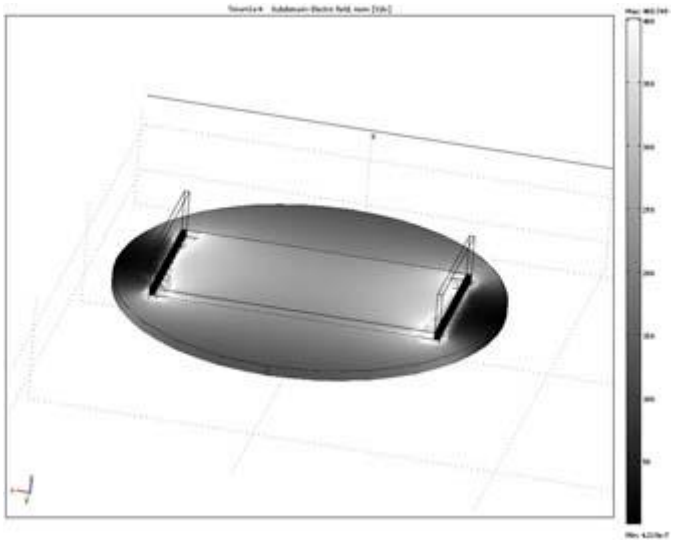

Figure 3. Value of the electric field at the peak current amplitude of 20 mA (culture medium, foam, dermis).

Electrical pattern (wave form, intensity, frequency of stimulation) shown in Figure 4 is the same as in the in vitro study published by Hinsenkamp et al. 1997 and the clinical study on chronic wound healing [Jercinovic et al., 1994]. The choice of daily stimulation is based on a review of the literature on the human application of electric and electromagnetic fields for chronic wound treatment [Vodovnik and Karba, 1992].

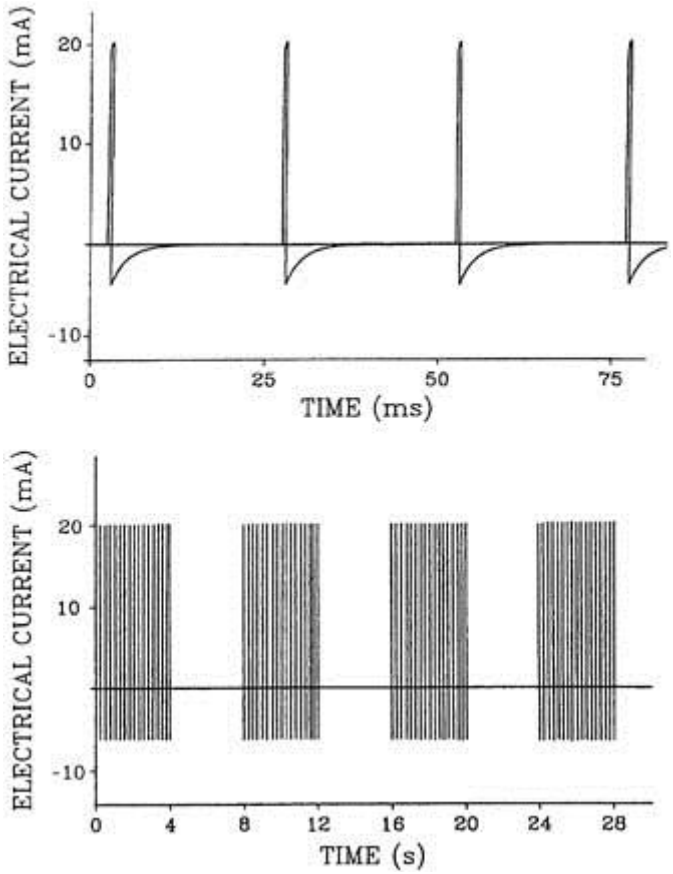

Figure 4. Electrical pattern used in the study. The output of the generator consists of a biphasic, asymmetric, charge-balanced current stimuli, with a repetition frequency of 40 Hz and a pulse width of 0.25 ms. The signal is presented with two different time scales. The graph on the top is related to the pulse train detailed below.

RNA Extraction

Total RNA was extracted in each sample condition from a pool of 12 explants. Each pool is homogenized with a rotor-stator and total RNA was extracted using a Qiagen RNeasy Mini Kit (Dusseldorf, Germany). The RNA quality was carefully assessed using the Agilent Technologies capillary electrophoresis system (Santa Clara, CA). The RNA quantities were determined by spectrometry using the NanoDrop Technologies spectrometer (Wilmington, DE).

Target Production and Hybridization

Microarray experiments and part of the data analysis were performed by PartnerChip (Evry, France) following the procedure recommended by Affymetrix® (Santa Clara, CA). The gene expressions of 38,500 human genes are analyzed using Affymetrix® microarray U133 Plus 2.0 chips. The protocol is repeated on three different patients. A total of 24 Affymetrix® chips are processed. Target was prepared and hybridized according to the Affymetrix® two-cycle technical protocol. Fluorescent images were detected in a GeneChip Scanner 3000 (Affymetrix®). Expression data and raw expression data (CEL files) were generated using GCOS software (Affymetrix®). Quality control was

assessed based on 3'/5'ratios of glyceraldehyde 3-phosphate dehydrogenase and β-actin control probe sets.

Normalization and Statistical Analysis

Normalization and statistical analysis of microarray data were performed using ArrayAssist® Expression Software (Agilent Technologies-Stratagene Products, La Jolla, CA) for the analysis of variance (ANOVA) and k-means analysis. ANOVA analyses were conducted on the results of control samples (J1control, J4control, J7control, J12control) and on the results of stimulated samples (J1control, J4stim, J7stim, J12stim). For the t-tests, P-values were performed individually for each comparison. Probe sets were defined as differentially expressed for one of the J(1, 4, 7, or 12)stim versus J1control or J(1, 4, 7, or 12)stim versus J(1, 4, 7, or 12)control time points, if the fold change (FC) was ≥2 or ≤ −2 and the P-value was ≤0.05 after unpaired t-test. Furthermore, probe sets were also found to be significant after ANOVA analyses were used for k-means clustering.

Real-Time rtPCR

To validate the microarray data, we evaluated the expression of the transcripts in the samples initially used for microarray analyses. The five genes proposed in our analysis have been verified on all RNA samples discussed. Only the times J7 and J12 for one patient have not been realized due to lack of RNA. Reverse transcription, preceded by treatment with DNase, was conducted using Invitrogen's Superscript II RT kit (Carlsbad, CA). Primers were selected using Primer3 software (www.frodo.wi.mit.edu) on FASTA sequence (NCBI Genebank, Bethesda, MD) and verified with NCBI BLAST software. Real-time rtPCR was performed using an Applied Biosystems 7500 Fast Real-Time PCR System and Power SYBR Green PCR Master Mix (Foster City, CA). A normalization of the expression of all transcripts was made to beta-2-microglobulin (B2M) and TATA box-binding protein (TBP). These two genes are part of a list proposed by Allen et al. 2008 as a reference for real-time rtPCR in human epidermal keratinocytes, and showed in our microarray results to have a similar expression in control and stimulated samples.

RESULTS

Microarray Analysis

After the normalization and statistical analysis ($P \leq 0.01$), 1131 genes for the control group and 471 genes for the stimulated group were regulated over time and grouped into nine clusters according to similar expression behaviors.

For the control group, the expression profiles of two clusters containing 19 and 99 genes indicated a general up-regulation of genes over time; two other clusters containing 29 and 76 genes indicated a general down-regulation of genes over time. Then, we used FatiGO (www.fatigo.org) and Gene Ontology (GO) [Gene Ontology Consortium, 2000] tools and the results show that 138 of these 223 genes are annotated in the gene ontology biological process at level 3 (Table 1). Terms at higher levels of the hierarchy describe more general functions or processes while terms at lower levels are more specific. The level at which a gene is annotated in the GO hierarchy depends on the extent of knowledge that the annotator has about its biological behavior.

Table 1. Results Obtained Through the FatiGO Tool Using the Gene Ontology Biological Process for 223 Genes of the Control Group

Level	GO Biological Process	Number of genes
level 3	cellular metabolic process (GO:0044237)	63
	primary metabolic process (GO:0044238)	58
	regulation of biological process (GO:0050789)	54
	cell communication (GO:0007154)	48
	macromolecule metabolic process (GO:0043170)	43
level 4	signal transduction (GO:0007165)	43
	regulation of cellular process (GO:0050794)	39
	system development (GO:0048731)	32
	anatomical structure morphogenesis (GO:0009653)	30
	biopolymer metabolic process (GO:0043283)	29
level 5	organ development (GO:0048513)	28
	cell surface receptor linked signal transduction (GO:0007166)	24
	cellular protein metabolic process (GO:0044267)	22
	cell development (GO:0048468)	19
	negative regulation of cellular process (GO:0048523)	17
level 6	tissue development (GO:0009888)	13
	regulation of nucleobase, nucleoside, nucleotide and nucleic acid metabolic process (GO:0019219)	13
	organ morphogenesis (GO:0009887)	12
	RNA biosynthetic process (GO:0032774)	12
	cell death (GO:0008219)	12
level 7	ectoderm development (GO:0007398)	12
	regulation of transcription (GO:0045449)	12
	transcription, DNA-dependent (GO:0006351)	12
	programmed cell death (GO:0012501)	9
	cyclic-nucleotide-mediated signaling (GO:0019935)	7
level 8	epidermis development (GO:0008544)	12
	regulation of transcription, DNA-dependent (GO:0006355)	12
	apoptosis (GO:0006915)	9
	transcription from RNA polymerase II promoter (GO:0006366)	9
	regulation of programmed cell death (GO:0043067)	8
level 9	regulation of apoptosis (GO:0042981)	8
	regulation of transcription from RNA polymerase II promoter (GO:0006357)	7
	angiogenesis (GO:0001525)	6
	positive regulation of programmed cell death (GO:0043068)	6
	G-protein signaling, coupled to cAMP nucleotide second messenger (GO:0007188)	6

For the stimulated group, the expression profiles of two clusters containing 11 and 41 genes indicated a general up-regulation of genes over time. Two other clusters containing 6 and 24 genes indicated a general down-regulation of genes over time, and 51 of these 82 genes are annotated in the gene ontology biological process at level 3 (Table 2).

Table 2. Results Obtained Through the FatiGO Tool Using the Gene Ontology Biological Process for 82 Genes of the Stimulated Group

Level	GO Biological Process	Number of genes
level 3	cellular metabolic process (GO:0044237)	30
	primary metabolic process (GO:0044238)	28
	cell communication (GO:0007154)	18
	macromolecule metabolic process (GO:0043170)	17
	regulation of biological process (GO:0050789)	16
level 4	signal transduction (GO:0007165)	15
	regulation of cellular process (GO:0050794)	13
	system development (GO:0048731)	11
	protein metabolic process (GO:0019538)	10
	biopolymer metabolic process (GO:0043283)	9
level 5	cell surface receptor linked signal transduction (GO:0007166)	9
	cellular protein metabolic process (GO:0044267)	8
	organ development (GO:0048513)	8
	cellular lipid metabolic process (GO:0044255)	8
	pregnancy (GO:0007565)	7
level 6	tissue development (GO:0009888)	7
	proteolysis (GO:0006508)	5
	G-protein coupled receptor protein signaling pathway (GO:0007186)	4
	protein modification (GO:0006464)	4
	RNA biosynthetic process (GO:0032774)	4
level 7	ectoderm development (GO:0007398)	7
	fatty acid metabolic process (GO:0006631)	4
	transcription, DNA-dependent (GO:0006351)	4
	regulation of transcription (GO:0045449)	3
	post-translational protein modification (GO:0043687)	3
level 8	epidermis development (GO:0008544)	7
	G-protein signaling, coupled to cyclic nucleotide second messenger (GO:000	3
	icosanoid metabolic process (GO:0006690)	3
	regulation of transcription, DNA-dependent (GO:0006355)	3
	transforming growth factor beta receptor signaling pathway (GO:0007179)	3
level 9	prostanoid metabolic process (GO:0006692)	
	G-protein signaling, coupled to cAMP nucleotide second messenger (GO:000	3
	osteoblast differentiation (GO:0001649)	2
	positive regulation of programmed cell death (GO:0043068)	1
	sphingoid catabolic process (GO:0046521)	1

Table 3. Number of Genes With an Expression That Is Modified in Control Samples at Days 4, 7, and 12 Compared to J1control, and the Number of Regulated Genes With an Expression That Is Modified in Stimulated Samples at Days 4, 7, and 12 Compared to J1control ($2 \leq FC \leq -2$ With $P \leq 0.05$)

	J_n Control / J_1 Control		J_n Stimulated /J_1 Control	
	Up Reg.	Down Reg.	Up Reg.	Down Reg.
J_4	93	203	315	626
J_7	389	313	228	397
J_{12}	397	609	441	505

Table 4. Number of Regulated Genes When Comparing Stimulated and Control Groups at Days 4, 7, and 12 ($2 \leq FC \leq -2$ With $P \leq 0.05$)

Stimulated / Control	J_4	J_7	J_{12}
Up Reg.	39	30	237
Down Reg.	265	190	259

The comparison of the list of significantly up- and down-regulated genes ($2 \leq FC \leq -2$ with $P \leq 0.05$) at the three stimulated times with their respective controls showed the following three up-regulated genes present during all experimental procedures at any sampling time:

- Thioredoxin reductase 1 (TXNRD1), FC: J4 = 2.02, J7 = 3.22, J12 = 2.34; P: J = 0.05, J7 = 0.05, J12 = 0.02.
- Activating transcription factor 3 (ATF3), FC: J4 = 2.49, J7 = 13.41, J12 = 9.28; P: J4 = 0.03, J7 = 0.05, J12 = 0.03.
- Membrane metallo-endopeptidase (MME), FC: J4 = 3.02, J7 = 5.53, J12 = 20.28; P: J4 = 0.005, J7 = 0.005, J12 = 0.04.

A further comparison of the gene list of J4 stimulated with J4 control shows that one gene on the up-regulated list is Dickkopf Homolog 1 (DKK1), FC = 4.42 and P = 0.01, and one gene on the down-regulated list is microtubule-actin cross-linking factor 1 (MACF1), FC = −2.66 and P = 0.008.

Real-Time rtPCR Validation

The genes controlled by real-time rtPCR show a good correlation with microarray results. Expression of these genes was presented as standardized ratios (±SEM) derived from the three different patients for microarray and real-time rtPCR results (Fig. 5).

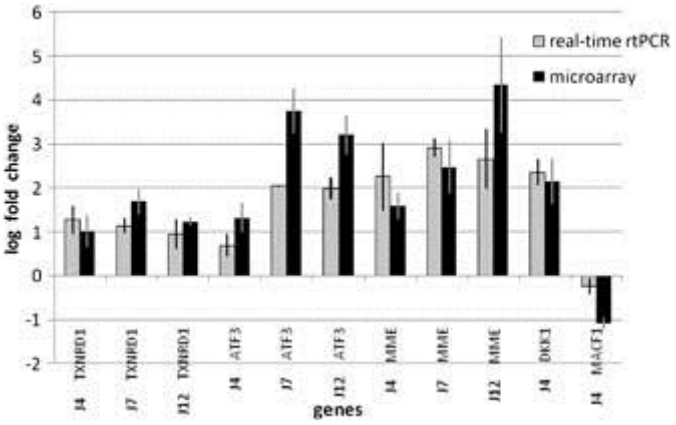

Figure 5. Comparison of microarray and real-time rtPCR results. The five genes used for discussion on microarray results have been validated on all RNA samples by real-time rtPCR. Real-time rtPCR and the microarray data are the average of the expression data obtained individually from the three patients. Standard error of the mean (SEM) was calculated for each gene.

DISCUSSION AND CONCLUSIONS

The results obtained with microarrays and confirmed by real-time rtPCR corroborate the results obtained previously on the same model using histology, thymidine labeling, and planimetry.

The robustness and quality of the results obtained by microarray technology were assessed by several papers. It was demonstrated that data from the two different technologies, microarray and real-time rtPCR, yield comparable results [Canales et al., 2006; Morey et al., 2006]. In the present study, regulation of all tested up-regulated genes was confirmed. The regulation of MACF1, the down-regulated gene in the microarray results, was also confirmed by real-time rtPCR but to a lesser extent.

Because our current results on cell cultures are totally consistent with previous in vitro and in vivo results mentioned in the Introduction Section, the cell mechanism studied by microarray and confirmed by real-time rtPCR seems to reflect in vivo situations with no significant interference from other physiological regulations.

The microarray analysis performed on epidermis skin cells exposed to ELF shows a significant up- or down-regulation in gene expression. The biological functions of genes concerned by a variation of their expression confirmed the macroscopic observation: an acceleration of differentiation at the expense of proliferation.

An analysis of gene expression at the three stimulated times compared with their three respective controls shows three genes (TXNRD1, ATF3, MME) up-regulated during the entire stimulation time. All play a part in cell proliferation and differentiation:

- TXNRD1, plays a role in the diminution of the proliferation in the embryo.
- ATF3, increases concentration in the process of differentiation of chondrocytes.
- MME, stops mitosis in G1 phase and plays a role in diminution of the proliferation.

Dickkopf Homolog 1 (DKK1) plays a role in the negative regulation of Wnt receptor signaling pathway [Gene Ontology Consortium, 2000; van der Horst et al., 2005]. The effect of the Wnt down-regulation was a reduction of cell proliferation [Pasca di Magliano et al., 2007] and an induction of terminal cell differentiation [Boyden et al., 2002; van der Horst et al., 2005]. Many Wnt effects are mediated through β-catenin, which accumulates in the cytoplasm and translocates to the nucleus if the Wnt pathway is activated. In the absence of Wnt signaling, β-catenin is phosphorylated by the serine/threonine kinases, casein kinase, and GSK-3 [Nusse, 2005].

DKK1 is regulated by the protein kinases, (SAPK)/c-Jun amino-terminal kinases (JNK) signaling cascades [Colla et al., 2007]. SAPK/JNK is activated by a variety of environmental stresses, such as UV or γ-radiation, inflammatory cytokines, and growth factors [Johnson and Nakamura, 2007; Weston and Davis, 2007]. Some environmental stresses are wave type and an ELF receiver is likely to complete the list of JNK pathway receptors or activators.

Microtubule-actin cross-linking factor 1 (MACF1) plays the role of a positive downstream regulator in the Wnt/β-catenin signaling pathway [Chen et al., 2006]. An active Wnt signaling pathway requires a translocation to the cell membrane of Axin and its associated proteins [Chen et al., 2006]. This translocation is impossible without the presence of MACF1. Down-regulation of MACF1 has the same purpose as the action of DKK1 on the Wnt molecule: an inactivation of the Wnt pathway and a decrease in β-catenin concentration.

None of our factual observations are involved in pathological manifestation but, through the activation of a normal physiological process, they may have potential therapeutic applications [Hinsenkamp et al., 1984, 1985b, 1993a,b]. Those applications are possible when an acceleration of cell differentiation is useful; for example, in the hypertrophic nonunion with pre-existing fibrocartilage, to accelerate the maturation of cartilage before ossification. This type of therapeutic application is probably responsible for the good prognosis observed in the treatment of tibia hypertrophic nonunions [Hinsenkamp et al., 1985b]. Other examples are pathologies where inhibition of the Wnt signaling pathway could be an interesting therapeutic target.

In the literature, some papers analyzed a possible effect of EMF on infantile leukemia. The most frequent leukemia in the child is acute lymphoblastic leukemia (ALL). Several papers concerning this subject indicate an activation of the Wnt signaling pathway in ALL [Khan et al., 2007] and an increase in the concentration of β-catenin [Chung et al., 2002]. Other articles showed inhibition of the Wnt signaling pathway as “an attractive target for the use of more specific therapies…” [Román-Gómez, 2007]. In our results, the β-catenin (present in the Wnt signaling pathway) and the Wnt signaling pathway are inhibited by the increased expression of the gene responsible for the synthesis of DKK1. A protocol is being established to investigate this hypothesis on blood cells.

Acknowledgements

The authors are grateful to C. Maenhaut and G. Dom of the Institut de Recherche Interdisciplinaire en Biologie Humaine et Moléculaire (IRIBHM) for their technical support in real-time rtPCR validation. We also thank P. Soularue and S. Baulande from PartnerChip, CEA Genopole, Evry, France, for their collaboration in the microarray analysis.

REFERENCES

Allen D, Winters E, Kenna PF, Humphries P, Farrar GJ. 2008. Reference gene selection for real-time rtPCR in human epidermal keratinocytes. J Dermsci 49: 217–225.

Boyden LM, Mao J, Belsky J, Mitzner L, Farhi A, Mitnick MA, Wu D, Insogna K, Lifton RP. 2002. High bone density due to a mutation in LDL-receptor-related protein 5. N Engl J Med 346(20): 1513–1521.

Canales RD, Luo Y, Willey JC, Austermiller B, Barbacioru CC, Boysen C, Hunkapiller K, Jensen RV, Knight CR, Lee KY, Ma Y, Maqsodi B, Papallo A, Peters EH, Poulter K, Ruppel PL, Samaha RR, Shi L, Yang W, Zhang L, Goodsaid FM. 2006. Evaluation of DNA microarray results with quantitative gene expression platforms. Nat Biotechnol 24(9): 1115–1122.

Chen H-J, Lin C-M, Lin C-S, Perez-Olle R, Leung CL, Liem RKH. 2006. The role of microtubule actin cross-linking factor 1 (MACF1) in the Wnt signaling pathway. Genes Dev 20: 1933–1945.

Chung EJ, Hwang SG, Nguyen P, Lee S, Kim JS, Kim JW, Henkart PA, Bottaro DP, Soon L, Bonvini P, Lee SJ, Karp JE, Oh HJ, Rubin JS, Trepel JB. 2002. Regulation of leukemic cell adhesion, proliferation, and survival by beta-catenin. Blood 100(3): 982–990.

Colla S, Zhan F, Xiong W, Wu X, Xu H, Stephens O, Yaccoby S, Epstein J, Barlogie B, Shaughnessy JD, Jr. 2007. The oxidative stress response regulates DKK1 expression through the JNK signaling cascade in multiple myeloma plasma cells. Blood 109(10): 4470–4477.

Gene Ontology Consortium. 2000. Gene ontology: Tool for the unification of biology. Nat Genet 25: 25–29.

Hinsenkamp M. 1994. Electromagnetic stimulation of osteogenesis and fractures consolidation. Brussels: Royal Academy of Belgium, Science Classes. 336 pp.

Hinsenkamp MG, Rooze MA. 1982. Morphological effect of electromagnetic stimulation on the skeleton of fetal or newborn mice. Acta Orthop Scand Suppl 196: 39–50.

Hinsenkamp M, Burny F, Donkerwolcke M, Coussaert E. 1984. Electromagnetic stimulation of fresh fractures treated with Hoffmann external fixation. Orthopedics 7: 411–416.

Hinsenkamp M, Rooze M, Noorbergen M, Tuerlinckx B. 1985a. Topography of EM exposure and its relationship to biological effects on tissues. In: ChiabreraA, NicoliniC, SchwanH, editors. Interactions Between Electromagnetic Fields and Cells. New York: Plenum Press. pp. 557–567.

Hinsenkamp M, Ryaby J, Burny F. 1985b. Treatment of non-union by pulsing electromagnetic field: European Multicenter Study of 308 cases. Reconstr Surg Traumat 19: 147–151.

Hinsenkamp M, Hauzeur JP, Sintzoff S. 1993a. Preliminary results in electromagnetic field treatment of osteonecrosis. Bioelectrochem Bioener 30: 229–235.

Hinsenkamp M, Hauzeur JP, Sintzoff S. 1993b. Results in electromagnetic fields (EMF) treatment of osteonecrosis. In: SchoutensA, ArletJ, GardeniersJ, HughesS, editors. Bone Circulation and Vascularization in Normal and Pathological Conditions. New York: Plenum Press. pp. 331–336.

Hinsenkamp M, Jercinovic A, de Graef C, Wilaert F, Heenen M. 1997. Effects of low frequency pulsed electrical current on keratinocytes in vitro. Bioelectromagnetics 18(3): 250–254.

Jercinovic A, Karba R, Vodovnik L, Stefanovska A, Kroselj P, Turk R, Dzidic I, Benko H, Savrin R. 1994. Low frequency pulsed current and pressure ulcer healing. IEEE Trans Rehab Eng 2(4): 225–233.

Jercinovic A, Hinsenkamp M, Scarceriaux B, Willaert F, De Graef C, Heenen M, Goldshmidt D. 1996. Effects of direct constant current (DC) on keratinocytes in vitro. Bioelectrochem Bioener 39: 209–214.

Johnson GL, Nakamura K. 2007. The c-jun kinase/stress-activated pathway: Regulation, function and role in human disease. Biochim Biophys Acta 1773(8): 1341–1348.

Khan NI, Bradstock KF, Bendall LJ. 2007. Activation of Wnt/beta-catenin pathway mediates growth and survival in B-cell progenitor acute lymphoblastic leukaemia. Br J Haematol 138(3): 338–348.

Morey J, Ryan J, Van Dolah F. 2006. Microarray validation: Factors influencing correlation between oligonucleotide microarrays and real-time PCR. Biol Proceed Online 8(1): 175–193.

Nusse R. 2005. Wnt signalling in disease and in development. Cell Res 15(1): 28–32.

Pasca di Magliano M, Biankin AV, Heiser PW, Cano DA, Gutierrez PJ, Deramaudt T, Segara D, Dawson AC, Kench JG, Henshall SM, Sutherland RL, Dlugosz A, Rustgi AK, Hebrok M. 2007. Common activation of canonical Wnt signaling in pancreatic adenocarcinoma. PLoS ONE 2(11): e1155.

Román-Gómez J. 2007. Epigenetic regulation of Wnt-signaling pathway in acute lymphoblastic leukemia. Blood 109(8): 3462–3469.

Rooze M, Hinsenkamp M. 1982. Histochemical modifications induced in vitro by electromagnetic stimulation of growing bone tissues. Acta Orthop Scand Suppl 196: 51–62.

Rooze M, Hinsenkamp M. 1985. In vivo modifications induced by electromagnetic stimulation of chicken embryos. Reconstr Surg Traumat 19: 87–92.

van der Horst G, van der Werf SM, Farih-Sips H, van Bezooijen RL, Löwik CW, Karperien M. 2005. Downregulation of Wnt signaling by increased expression of Dickkopf-1 and -2 is a prerequisite for late-stage osteoblast differentiation of KS483 cells. J Bone Miner Res 20(10): 1867–1877.

Vodovnik L, Karba R. 1992. Treatment of chronic wounds by means of electric and electromagnetic fields. Part 1. Literature review. Med Biol Eng Comput 30: 257–266.

Weston CR, Davis RJ. 2007. The JNK signal transduction pathway. Curr Opin Cell Biol 19(2): 142–149.